Healthy aging and muscle function are positively associated with NAD+ abundance in humans

Janssens, George E.; Grevendonk, L.; Zapata Perez, Ruben; Schomakers, Bauke V.; den Bosch, Johan de Vogel-van; Geurts, J.; van Weeghel, Michel; Schrauwen, Patrick; Houtkooper, Riekelt H. L.; Hoeks, Joris

Published in:
Nature Aging

DOI:
10.1038/s43587-022-00174-3

Published: 17/02/2022

Document Version
Peer reviewed version

Citation for pulished version (APA):
Janssens, G. E., Grevendonk, L., Zapata Perez, R., Schomakers, B. V., den Bosch, J. D. V., Geurts, J., van Weeghel, M., Schrauwen, P., Houtkooper, R. H. L., & Hoeks, J. (2022). Healthy aging and muscle function are positively associated with NAD+ abundance in humans. *Nature Aging*, *2*, 254-263. https://doi.org/10.1038/s43587-022-00174-3

Healthy aging and muscle function are positively associated with NAD^+ abundance in humans

Georges E. Janssens[1*], Lotte Grevendonk[2,3*], Ruben Zapata Perez[1], Bauke V. Schomakers[1,4], Johan de Vogel-van den Bosch[5], Jan M. W. Geurts [6], Michel van Weeghel[1,4], Patrick Schrauwen[2,3], Riekelt H. Houtkooper[1,§], Joris Hoeks[2,3,§].

[1] Laboratory Genetic Metabolic Diseases, Amsterdam UMC, University of Amsterdam, Amsterdam Gastroenterology, Endocrinology, and Metabolism, Amsterdam Cardiovascular Sciences, Meibergdreef 9, 1105 AZ Amsterdam, The Netherlands
[2] Department of Nutrition and Movement Sciences, NUTRIM School of Nutrition and Translational Research in Metabolism, Maastricht University, 6200 MD Maastricht, The Netherlands
[3] TI Food and Nutrition, PO Box 557, 6700 AN, Wageningen, The Netherlands.
[4] Core Facility Metabolomics, Amsterdam UMC, University of Amsterdam, The Netherlands
[5] Danone Nutricia Research, P.O. Box 80141, 3508 TC Utrecht, The Netherlands.
[6] FrieslandCampina, 3818 LE Amersfoort, The Netherlands
[*]Equal contribution

[§]Correspondence:
Joris Hoeks: j.hoeks@maastrichtuniversity.nl
Riekelt H. Houtkooper: r.h.houtkooper@amsterdamumc.nl

Abstract

Skeletal muscle is greatly affected by aging, resulting in a loss of metabolic and physical function. However, the underlying molecular processes and how (lack of) physical activity is involved in age-related metabolic decline in muscle function in humans is largely unknown. Here we compared, in a cross-sectional study, the muscle metabolome from young to older adults, whereby the older adults were either exercise-trained, had normal physical activity levels, or were physically impaired. Nicotinamide adenine dinucleotide (NAD^+) was one of the most prominent metabolites that was lower in older adult humans, in line with preclinical models. This lower level was even more pronounced in impaired older individuals, and conversely, exercise-trained older individuals had NAD^+ levels that were more similar to those found in the young. NAD^+ abundance positively correlated with average steps-per-day and mitochondrial and muscle functioning. Our work suggests that a clear association exists between NAD^+ and health status in human aging.

Keywords

Healthy longevity, muscle aging, metabolomics, exercise, NAD^+

Abbreviations

KYNA	Kynurenic acid
KYNU	Kynurenine
NaAD	Nicotinic acid adenine dinucleotide
NAD^+	Nicotinamide adenine dinucleotide
NAM	Nicotinamide
NaMN	Nicotinic acid mononucleotide
NAMPT	Nicotinamide phosphoribosyltransferase
NMN	Nicotinamide mononucleotide
NR	Nicotinamide riboside
NRH	Dihydronicotinamide riboside
PARPs	Poly(ADP-ribose) polymerases
PBMC	Peripheral blood mononuclear cell
PPP	Pentose phosphate pathway
PRPP	Phosphoribosyl pyrophosphate
QA	Quinolinic acid
SPPB	Short physical performance battery
Trp	L-Tryptophan
UPLC-HRMS	Ultra-high performance liquid chromatography high-resolution mass spectrometry

Introduction

Over the past few decades, remarkable achievements in healthcare have led to a dramatic increase in the average life expectancy in most economically developed countries[1,2]. However, this increased lifespan is not paralleled by an increase in health span, as aging is accompanied by the development of various age-related pathologies including metabolic disorders[3]. Understanding and targeting the aging process itself, rather than treating the symptoms of these age-related pathologies, may be the most effective strategy to prevent or counteract aging-related health decline[4].

The development of many age-related diseases has been associated with disturbances in mitochondrial metabolism, a hallmark of the aging process[5]. In that context, we and others have previously shown in both muscle and liver that pathways involved in oxidative phosphorylation (OXPHOS), fatty acid oxidation, and mitochondrial biogenesis are impaired in aged mice[6,7]. In addition, we also reported that aged *C. elegans* are characterized by a prominent accumulation of most fatty acid species, which appeared to be controlled, at least in part, by the mitochondrial metabolic regulator AMPK[8]. Together, these preclinical studies highlight that alterations in various metabolic pathways, particularly within mitochondrial metabolism, are linked to the aging process and could therefore explain age-related metabolic complications.

Skeletal muscle is highly affected by the aging process[9] and age-induced loss of skeletal muscle mass and function have been related to mobility impairments[10,11], an increased risk of falls[12,13] and physical frailty[14]. Aging is also associated with a decline in muscle metabolism, as exemplified by a decrease in insulin sensitivity, metabolic inflexibility, increased oxidative damage, and the occurrence of skeletal muscle mitochondrial dysfunction[15–17]. On the other hand, regular exercise positively impacts muscle metabolism and function, and regular exercise training has been shown to protect against aging-induced deterioration of muscle health[18,19].

Based on these considerations, the aims of the present study were to investigate the muscle metabolome comparing young and aged individuals, and to identify how differences in the aged individuals may be associated to muscle and mitochondrial function. This comparison was expanded upon by evaluating changes in three groups of older individuals recruited according to their 'muscle health' states; aged individuals who 1) were exercise-trained (‘trained’ older adults), 2) who possessed normal physical activity abilities (‘normal’ older adults), or 3) who displayed an impaired physical function (‘impaired’ older adults). Our results show that nicotinamide adenine dinucleotide (NAD^+) was one of the most depleted metabolites with age and that age-related NAD^+ depletion followed a 'healthy aging' trend, whereby physically impaired older individuals were marked by significantly lower NAD^+ levels and exercise-trained older individuals could maintain NAD^+ abundance to levels nearly as high as in the young. Furthermore, we found that in the older adults NAD^+ muscle abundance positively correlated with muscle and mitochondrial health parameters. Taken together, these results provide a first-time account that NAD^+ is lower in aging human muscle and that NAD^+ abundance is directly associated to the healthy aging state of the individual.

Results

The metabolome of human muscle aging

In order to better understand which metabolites were associated to aging and to establish a 'healthy aging' muscle signature, we turned to an extensively characterized cohort of young and aged individuals, which we previously established (clinicaltrials.gov identifier NCT03666013). This mixed-gender cohort consisted of individuals that were either young (n=12) or belonged to one of three aged groups; trained older adults (n=17), older adults with normal physical activity levels (n=17), or physically impaired older adults (n=6). Participants were categorized into different study groups based on age, their levels of self-reported physical exercise training, and their levels of physical function. Participants were considered normally physically active if they completed no more than one structured exercise session per week. Older participants were considered exercise-trained if they engaged in at least three structured exercise sessions of at least one hour each per week for an uninterrupted period of at least one year prior to inclusion. Older participants were classified as physically impaired in case of a Short Physical Performance Battery (SPPB) score of ≤ 9 (Supplemental Table 1). Upon inclusion, further details on habitual physical activity levels were obtained using accelerometry. Over the course of five days, young individuals took an average of ~10K steps per day and spent 2.5% of their active time in high-intensity activities (Figure 1A). The normal older adults group possessed similar (~10K steps/day and 2.2% active time in high-intensity activities), ensuring that changes observed between these groups were age-related rather than fitness-related. Meanwhile, trained older adults were more active (~13K steps/day on average) with more time spent in high-intensity activities (5.2%), whereas the physically impaired older adults displayed a lower average daily step count (~6K) and a lower amount of their active time spent in high-intensity activities (1.0%) (Figure 1A).

Using the muscle biopsies collected from each participant in these groups, we performed ultra-high performance liquid chromatography coupled to high-resolution mass spectrometry (UPLC-HRMS)-based metabolomics (Supplemental Table 2). The results were used to establish a baseline understanding of the differences occurring between young and older adults with normal and equivalent levels of physical activity, taking into account all 137 metabolites we were able to annotate. Comparing the muscle metabolomes of these two groups using a principal component analysis, we found a general separation between the groups to exist within the first two principal components, suggesting aging to impart large changes in the muscle metabolome (Extended Data Figure 1A).

To better understand what metabolites were contributing to the differences occurring with aging, we compared the accumulated and depleted metabolites (Figure 1B, Extended Data Figure 1B). We found a clear signature of changes to occur with normal aging (Figure 1B). Intriguingly, when considering the top five metabolites either accumulating or depleting in older vs. young adults with normal and equal physical activity, we found older adults to possess higher levels of ophthalmic acid, an oxidative stress marker[20,21], and dihydroxyacetone-phosphate and 3-methoxytyramine, two metabolite families negatively associated to mitochondrial respiration[22,23]. Moreover, we found a significant age-related decline of NAD^+ to occur with aging. Together, these changes suggest an age-related change in oxidative metabolism in skeletal muscle (Figure 1C).

NAD^+ abundance is directly related to healthy aging muscle

Having established the metabolic changes occurring with aging in muscle, which pointed towards alterations in oxidative metabolism, we next asked which of these differences were not only linked to aging but were also related to muscle health levels. To do so, we ranked metabolites based on the degree to which their abundance level followed a health trend with the four groups, from young adults to trained older adults, to normally active older adults, to physically impaired older adults. This approach was designed to highlight metabolites that may be lower with normal aging, with a decline that is either (nearly) absent with regular exercise training or exacerbated by belonging to a physically impaired aging group. Plotting these correlations against the normal aging changes served to highlight the age-related changes that are important also on a health and exercise related axis. Remarkably, we found that changes in normal older adults and changes that follow a 'health trend' are highly correlated, implying that most metabolic changes that occur with age in the muscle can be reversed with regular exercise training (Figure 2A).

In line with this observation, we found that NAD^+ was not only one of the most depleted molecules in older adults when compared to young individuals, (Figure 1C) but also displayed the strongest association to healthy aging (Figure 2A). Indeed, age-related NAD^+ differences (Figure 1B) were exacerbated in the impaired older adults (Figure 2B, Extended Data Figure 2A). Furthermore, according to the Venn diagram analysis, significant age-related lower NAD^+ levels were only found to be in common between the normal aging and the impaired aging groups (Extended Data Figure 2B). Meanwhile, the trained older adults group possessed levels of NAD^+ comparable to the levels if NAD^+ present in the young (Figure 2B, Extended Data Figure 2B).

Interestingly, we found ophthalmic acid, a marker of oxidative stress and one of the top-five accumulated metabolites (Figure 1C), to display the opposite trend as observed for NAD^+, namely, a higher abundance in older adults compared to young that became exacerbated in physically impaired older adults and was attenuated in trained older adults (Figure 2A, Figure 2C). In addition, we found that oxiglutathione, another marker of oxidative stress, followed the same trend as ophthalmic acid (Figure 2A), suggesting that NAD^+ depletion with aging may occur in parallel with increased ROS production.

Modulation of the NAD^+-pathway with aging

Our untargeted metabolomics data pointed towards oxidative metabolism as a central player in aging muscle. Having observed that NAD^+ was both lower in normal aging and also possessed the strongest correlation to healthy aging, we next asked how the NAD^+-pathway itself was modulated in our older adults relative to the young. To do so, we considered all NAD^+-related metabolites (Extended Data Figure 3A-L) and mapped out how they changed in each older adult group relative to young, onto the NAD^+ synthesis pathway (Figure 3). The depletion of NAD^+, observed per aged group, was mirrored by a depletion of NADH, although to a lesser extent (Figure 3), and the ratio of NAD^+ to NADH appeared to be maintained across the groups in general (Extended Data Figure 4A). Furthermore, we observed a lack of modulation of $NADP^+$ and NADPH in the aged

groups, which points towards an aging and exercise-dependent modulation of NAD(H), but not of their phosphorylated forms.

Having established NAD(H)'s associations to healthy aging, we next turned our attention to other metabolites involved in NAD^+ *de novo* synthesis and recycling. We found a strong correlation between kynurenic acid accumulation and the healthy aging trend (Figure 3, Extended Data Figure 3B). Kynurenic acid is produced by kynurenine aminotransferase (KAT)-mediated irreversible transamination of kynurenine, a downstream metabolite of tryptophan in the NAD^+ *de novo* synthesis pathway, or through ROS-mediated oxidative degradation of kynurenine[24]. This latter explanation is in line with our previously noted increase in the oxidative damage markers ophthalmic acid and oxiglutathione[20,21] in the older adults (Figure 2A, Figure 2C), supporting the hypothesis that kynurenic acid is produced via ROS-mediated degradation of kynurenine.

To further explore the metabolomic responses involved in oxidative stress, we mapped out the glutathione and oxiglutathione pathway, which are generated by precursors such as glutamate and glycine (Extended Data Figure 4B). Since electrons from glutathione are used to quench free radicals, forming oxiglutathione in the process, the glutathione / oxiglutatione ratio can be indicative of oxidative stress[20,21]. This may occur by either a decrease in glutathione and/or increase in oxiglutathione, ultimately producing a decrease of the glutathione / oxiglutathione ratio. As noted, ophthalmic acid is a marker for glutathione synthesis, reflecting oxidative stress[20,21]. In addition to the significant increase in ophthalmic acid previously noted (Figure 2C), we found a significant increase in oxiglutathione for all aged groups relative to young subjects, resulting in a significant decrease in the glutathione / oxiglutathione ratio (Extended Data Figure 4B). While a trend was visible for lower oxiglutathione and thereby a higher glutathione / oxiglutathione ratio in athletic older adults relative to impaired older adults, these were not significant (Extended Data Figure 4B). Although these reported ratios do not directly correspond to biological ratios of these metabolites, due to different ionization efficiencies in the mass spectrometer between glutathione and oxiglutathione, the observed changes in this analytical glutathione/oxiglutathione ratio between groups are still physiologically meaningful. We also noted that glutamate and glycine were similar across groups (Extended Data Figure 4B). While cysteine could not be determined in these samples, our data suggests that glutathione demand is increased due to an increased oxidative milieu that occurs with aging and that this is possibly depleting cysteine stores.

NAD^+ relates to mitochondrial function and muscle health

Our cohort possessed extensive phenotyping of muscle health parameters, which offered an unprecedented opportunity to better understand how the age-related decline of NAD^+ related to various outcomes of muscle health, an unexplored domain in human physiology. To address this, we performed a cross correlation of the abundances of NAD^+-related metabolites to muscle-related parameters previously measured (clinicaltrials.gov identifier NCT03666013)[25] in three older adult groups (Extended Data Figure 5A). Phenotypical parameters consisted of molecular measurements of mitochondrial abundance (OXPHOS subunit abundances), mitochondrial respiration (oxygen consumption measurements in permeabilized muscle fibers), and *in vivo* mitochondrial function (PCr recovery), in addition to physiological parameters, including

muscle energetics (net exercise efficiency %), muscle volume (MRI), muscle strength (isokinetic function), and habitual physical activity (accelerometry) (Extended Data Figure 5B). By comparing and focusing our analyses on the metabolite abundances that correlate or anti-correlate with these molecular and physiological parameters, we reasoned that a correlation network could map the landscape of NAD^+-related interactions associated with healthy muscle aging.

This approach revealed that a network existed that strongly linked NAD^+ metabolites to aging muscle function. Intriguingly, within this network kynurenic acid acted as a hub of negative associations, while NAD^+ was positively associated with many functional parameters of the muscle (Figure 4A). For example, we found that NAD^+ abundance had a strong positive association to maximum ADP-stimulated (state 3) mitochondrial respiration (Figure 4B). Likewise, and quite remarkably, NAD^+ abundance in muscle was also correlated to the average daily step count (Figure 4C). Meanwhile, when considering negative correlations, we observed that kynurenic acid was inversely associated with isokinetic muscle strength (Figure 4D) and kynurenine was inversely associated with net exercise efficiency (Figure 4E). Taken together, this approach revealed a first-time view of the significant relationship the NAD^+ pathway has to the healthy aging muscle functioning of older individuals.

Numerous preclinical studies have indicated NAD^+ depletion as the primary cause of disease and disability during aging[26]. While we have seen that boosting NAD^+ metabolism in humans only induced very minor physiological changes[27–29], increasing NAD^+ in animal models improved, amongst others, muscle recovery, endurance capacity, mitochondrial function, oxidative metabolism, insulin sensitivity, and lipid profiles, and extended lifespan[17,30–36]. In line with these preclinical studies, our NAD^+-related metabolite and muscle physiology network supports that NAD^+ abundance is indeed an indicator of muscle health status in aging individuals.

Discussion

In the current study we investigated age-related muscle metabolomic changes comparing young and aged individuals. We identified how metabolomic differences in aged individuals relate to muscle and mitochondrial function by evaluating changes across a healthy (muscle) aging trend. Out of the 137 detected metabolites, NAD^+ was one of the most depleted metabolites upon aging, a finding which itself fills a void in the literature between preclinical animal research and clinical human research. Namely, to date, very few studies have established that NAD^+, which declines in laboratory animals, also declines in human tissues[37]. Moreover, our study found that not only is NAD^+ lower in aged adults compared to young adults, but the levels are associated with the health state of the aged individual. Specifically, it is lowest in the impaired older adults whereas exercised-trained older adults show similar levels as young individuals, and NAD^+ abundance was directly positively associated with mitochondrial respiration and physiological muscle functioning when considering all individual older adults.

In this study, the young and normal aging groups were not engaged in structured exercise activities, and both recorded approximately 10,000 steps daily. Although this is well above the general recommendations[38], our results suggest that maintaining a healthy physical activity level in older people comparable to the young is not sufficient to prevent an age-related decline in NAD^+. However, endurance-trained older participants

who had 12,500 steps/day and performed at least three exercise-training sessions per week, did not show the lower NAD^+ levels that occurred during normal aging. In contrast, physically impaired older adults in our study averaged less than 7,500 steps/day, reflecting a more sedentary lifestyle relative to the other participants[39]. The differences in habitual physical activity levels between the aging groups were directly reflected in NAD^+ metabolism, whereby quite strikingly, daily step counts correlated strongly with muscle NAD^+ levels. Taken together, our results suggest that the best therapy to maintain youthful and physiologically important levels of NAD^+ during aging may simply involve highly structured exercise regimes, though this may not be realistic for all aging individuals.

While an age-related decline of NAD^+ and the benefits of boosting NAD^+ levels have been extensively demonstrated in model organisms[17,30–36], relatively little evidence exists relating NAD^+ to aging and health in humans[37]. To our knowledge, to date, an age-related decline in NAD^+ levels in humans has only been demonstrated to occur in the brain (using magnetic resonance spectroscopy)[40,41] and pelvic skin samples (measured spectrophotometrically)[42]. Here we further demonstrate that NAD^+ is lower with human aging in skeletal muscle. Interestingly, it has previously been shown in human skeletal muscle that levels of nicotinamide phosphoribosyltransferase (NAMPT), the rate-limiting enzyme in the NAD^+ salvage pathway, decreases with aging and that both aerobic and resistance exercise training can increase NAMPT levels[43]. While the study was not designed to directly measure NAD^+, the findings are in line with ours, suggesting that a lifestyle with exercise is associated with higher NAD^+ levels compared to a lifestyle without intensive exercise in older adults.

Transcriptomic and metabolomic studies in human skeletal muscle have extensively been studied in the context of frailty and sarcopenia, with key findings demonstrating changes in mitochondrial function, muscle growth, and cell turnover[44–46]. One study has demonstrated that NAD^+ (measured enzymatically) and mitochondrial oxidative capacity is decreased in sarcopenic older men relative to age-matched controls[47]. While the study was not designed to investigate whether older adults had lower levels of NAD^+ than young individuals in the first place, their findings are in line with our findings that impaired older adults have lower NAD^+ levels compared to normal older adults. Taken together, our work complements these recent findings and incorporates both young and old individuals, possessing both athletic and impaired aging states, to solidify our understanding of NAD^+ in skeletal muscle healthy aging.

A number of open questions accompany our findings. Firstly, we noted reduced ADP-ribose in trained older adults relative to young adults despite comparable NAD^+ levels (Figure 3, Extended Data Figure 3). This difference was not significant in normal and impaired older adults. Since ADP-ribose is produced in part through the activity of NAD^+ consumers, a depletion of ADP-ribose may suggest a reduction in the activity of NAD^+ consumers in trained older adults, and therefore may indirectly result in higher levels of NAD^+. Results from other studies, however, point towards increased NAD^+ recycling via NAMPT upon exercise[43,48]. Since NAMPT requires phosphoribosyl pyrophosphate (PRPP), which can be synthesized from ADP-ribose by the activities of ADPrases[49,50] and the PRPP synthase[51], the depletion in ADP-ribose we observe may also fit the hypothesis that ADP-ribose is being utilized to produce NAD^+. More research is required to distinguish whether reduced consumption, or increased production, is the cause of the differences we observed in NAD^+ levels between the age groups. Secondly, we observed an increase in kynurenine and kynurenic acid with aging, which was negatively

correlated to muscle function in our participants. Kynurenic acid accumulates with aging in human cerebrospinal fluid[52], underlies learning and memory impairment associated with aging in *C. elegans*[53], and has been implicated in many diseases associated with inflammation and aging ("inflammaging")[54–56]. Furthermore, it has recently been shown that trained muscle uses kynurenine metabolism to increase bioenergetic efficiency[57]. An open question emerges therefore on how kynurenine may mechanistically relate, rather than simply being associated, to the efficiency of muscle contraction in aging observed in our study. Of third consideration, our study focused on the NAD^+ pathway due to its prominent association to health in our data, however a number of other metabolites emerged from our analyses and deserve further investigation. These include, for example, hydroxyphenyllactic acid, aspartate, beta-alanine, and 3-methoxytyramine, amongst others, which we found to change in a health-dependent manner with aging. It must therefore be noted that other factors are also at play, and not just NAD^+, in the relationship between muscle function and aging. Of fourth consideration, several studies using NAD^+ precursors to boost NAD^+ levels did not find associations with NAD^+ and either skeletal muscle or mitochondrial functioning, suggesting factors in addition to NAD^+ alone may be playing a role in our observations[58,59].

Finally, several limitations should be considered in relation to our study. Firstly, while the SPPB scores largely defined the placement of individuals in our different aged health groupings, variations within the groups still exist. As a result, the group-based analyses (such as in Figure 3) may have a lower resolution to detect differences, compared to the ungrouped analyses (such as in Figure 4). Secondly, the power calculation to determine the number of study participants was performed using the original primary outcome of the cohort studied (NCT03666013)[25], which was the rate of *ex vivo* mitochondrial respiration. Therefore, the number of samples used in this study was based on this calculation and the sample availability at the time we performed metabolomics. Consequentially, several groups had low numbers of participants (such as in the impaired aging group), which may make subtler differences in the metabolome difficult to detect, and the low sample number makes it virtually impossible to meaningfully stratify the results across gender, BMI, and other demographic measures. Nonetheless, despite these low numbers and diverse study population, we still found significant differences in the NAD^+ pathway, which serves to reinforce the fact that NAD^+ depletion in muscle is a profound phenotype of human aging. Thirdly, our metabolomics were performed on muscle biopsies, which is an inherently heterogeneous sample type, both within and between individuals. This includes heterogeneity at the level of muscle fiber type (e.g. endurance trained older individuals may have more Type I rather than Type II muscle fibers[60–62]), and intracellular heterogeneity (e.g. NAD^+ is present in both cytosolic and mitochondrial subcellular locations, which can be relevant for health[63]). Therefore, our study could not resolve whether the changes in NAD^+ abundance were due to ratio shifts in muscle fiber types, or specific changes in subcellular NAD^+ pools. Further research is needed to resolve this. Finally, of fourth consideration, our work reports on a cross-sectional study population, rather than a prospective study. Due to its cross-sectional design our study does not prove that exercise can prevent the aging-related decline in muscle NAD^+ levels, and a follow-up prospective study would be required to address this. Furthermore, our work does not eliminate the possibility that if the physiology of an individual is such that they possess higher NAD^+ when old, they may be predisposed to higher activity levels (reverse causation possibility).Therefore causal involvement is difficult to conclude.

In summary, our study advances our understanding of the relevance of NAD^+ metabolism to human muscle aging, characterizing NAD^+ metabolism in extensively phenotyped young and older adults. Specifically, novel findings of our study include that (i) aging is associated with lower levels in skeletal muscle's NAD^+ abundance, occurring despite older adults maintaining adequate physical activity, (ii) lower NAD^+ levels relate to impaired aging and a high-intensity athletic aging lifestyle results in muscle NAD^+ levels similar to those seen in the young, and (iii) NAD^+ metabolism strongly correlates with human skeletal muscle health during aging as assessed through mitochondrial and physical functioning, whereby the average daily step count an older adult takes directly associates with their muscle NAD^+ levels. Together this work affirms the relation of NAD^+ with overall health status in aging individuals and highlights the NAD-pathway as a promising target to promote healthy aging in humans.

Methods

Human subjects and procedures

Fifty-two participants, including 12 young (7 male and 5 female) and 40 older individuals (23 male and 17 female) were recruited in the community of Maastricht and its surroundings through advertisements at Maastricht University, in local newspapers, supermarkets, and at sports clubs. The study protocol was approved by the institutional Medical Ethical Committee and conducted in agreement with the declaration of Helsinki. All participants provided their written informed consent, and the study was registered at clinicaltrials.gov with identifier NCT03666013. Participants received a fee to compensate for their time investment along with a compensation for travel expenses. Data collection and analysis were not performed blind to the conditions of the experiments. Physiological data from this cohort has been reported in our previous study as part of a different analysis[25]. Fully annotated demographic data (e.g., sex, BMI, etc.) for each individual participant is available as supplementary material therein. Prior to inclusion, all subjects underwent a medical screening that included a physical examination by a physician and an assessment of physical function using the Short Physical Performance Battery (SPPB), comprised of a standing balance test, a 4-m walk test, and a chair-stand test. After the screening procedure, participants were categorized into to the following study groups: Young individuals with normal physical activity (Y, 20 – 30 years), older adults with normal physical activity (NA, 65 – 80 years), athletic older adults (AA, 65 – 80 years) and physically impaired older adults (IA, 65 – 80 years). Participants were considered normal, physically active (NA) if they completed no more than one structured exercise session per week. Participants were considered trained (AA) if they engaged in at least 3 structured exercise sessions of at least 1 hour each per week for an uninterrupted period of at least one year. Participants were classified as older adults with impaired physical function (IA) in case of an SPPB score of ≤ 9. The SPPB score was calculated according to the cut-off points determined by[64]. Subject characteristics are summarized in Supplemental Table 1.

Muscle biopsy

At 9 AM, after an overnight fast from 10 PM the preceding evening, a muscle biopsy was taken from the *m. vastus lateralis* under local anesthesia (1.0% lidocaine without epinephrine) according to the Bergström method[65]. Part of the biopsy was immediately placed in an ice-cold preservation medium (BIOPS, OROBOROS Instruments, Innsbruck, Austria) and used for the preparation of permeabilized muscle fibers and measurement of *ex vivo* mitochondrial oxidative capacity, as described earlier [66,67]. The remaining part of the muscle biopsy was immediately frozen in melting isopentane and

stored at –80°C until further analysis.

Mitochondrial respiration

Permeabilized muscle fibers (~2.5 mg wet weight) were used for the assessment of mitochondrial capacity using a 2-chamber oxygraph (OROBOROS Instruments), according to[68]. To prevent oxygen limitation, the oxygraph chambers were hyper-oxygenated up to ~400 µmol/L O_2. Subsequently, two different multi-substrate/inhibition protocols were used in which substrates and inhibitors were added consecutively at saturating concentrations. State 2 respiration was measured after the addition of malate (4 mmol/L) plus octanoyl-carnitine (50 µmol/L) or malate (4 mmol/L) plus glutamate (10 mmol/L). Subsequently, an excess of 2 mmol/L of ADP was added to determine coupled (state 3) respiration. Coupled respiration was then maximized with convergent electron input through Complex I and Complex II by adding succinate (10 mmol/L). Finally, the chemical uncoupler carbonylcyanide-4-(trifluoromethoxy)-phenylhydrazone (FCCP) was titrated to assess the maximal capacity of the electron transport chain (state 3u respiration). The integrity of the outer mitochondrial membrane was assessed by the addition of cytochrome C (10 µmol/L) upon maximal coupled respiration. If cytochrome C increased oxygen consumption > 15%, the measurement was excluded to assure the viability and quality of the respiration measurement. All measurements were performed in quadruplicate.

Mitochondrial content

Mitochondrial content was assessed by mitochondrial OXPHOS protein expression using western blot analyses in Bioplex-lysates of human muscle tissue as previously described[69]. Equal amounts of protein were loaded onto 4–12% Bolt gradient gels (Novex, Thermo Fisher Scientific, Bleiswijk, The Netherlands). Proteins were transferred to a nitrocellulose membrane using the Trans-Blot Turbo transfer system (Bio-Rad Laboratories, Hercules, CA, USA). Primary antibodies contained a cocktail of mouse monoclonal antibodies directed against structural subunits of human OXPHOS (dilution 1:10,000; ab110411, Abcam, Cambridge, UK). The hOxPHOS proteins were detected using secondary antibodies conjugated with IRDye680 or IRDye800 and were quantified with a CLx Odyssey Near-Infrared Imager (Li-COR, Westburg, Leusden, The Netherlands).

Magnetic resonance imaging and spectroscopy (Pcr recovery and muscle volume)

All MR experiments were performed on a 3T whole-body MRI scanner (Achieva 3T-X; Philips Healthcare, Best, The Netherlands). Participants were positioned supine in the MR scanner to determine muscle volume with a series of T1-weighted images of the upper leg (slice thickness = 10.0 mm, no gap between slices, in‐plane resolution = 0.78 x 0.78 mm). A custom-written MATLAB 2016a script (The Mathworks Inc. Natick, MA, USA) was used to segment adipose tissue and muscle and quantify muscle volume semi-automatically. The muscle segmentation was performed in consecutive slices between the lower end of the *m. rectus* femoris and the lower end of the *m. gluteus maximus*. Phosphorus magnetic resonance spectroscopy (^{31}P-MRS) was performed to measure *in vivo* mitochondrial function in *m. vastus lateralis,* as previously described [70], using a 6 cm surface coil. A series of 150 unlocalized ^{31}P-spectra was acquired using the following parameters: single acquisitions (NSA = 1); repetition time (TR) = 4000 ms; spectral bandwidth = 3000 Hz; number of points = 1024. The 150 spectra were divided into 10 spectra at rest, 70 spectra during knee-extension exercise, and 70 spectra during recovery. Exercise within the scanner was performed to an auditory cue (0.5 Hz) in a

custom-built knee-extension device with adjustable weight. The intensity was chosen to correspond to 50–60% of the predetermined maximum weight. Spectra were analyzed with a custom-made MATLAB 2016a script. PCr, ATP, and inorganic phosphate peaks were fitted, and pH was determined. The PCr recovery was fitted with a mono-exponential function and the rate constant (k in s^{-1}) was determined as previously described[70]. The rate constant k of PCr resynthesis is almost entirely dependent on ATP produced by oxidative phosphorylation and can be used as a parameter of *in vivo* oxidative capacity[71].

Muscle function (exercise efficiency)
Exercise efficiency was measured during a 1-hour submaximal exercise bout in the fasted state on an electronically-braked cycle ergometer. The submaximal cycle test was performed at 50% of Wmax, as determined during a maximal aerobic cycling test. To calculate exercise energy expenditure (EEE), O_2 consumption and CO_2 production were recorded using indirect calorimetry for 15 minutes at two timepoints, T = 15 and T = 45 (Omnical, IDEE, Maastricht, The Netherlands). EEE was calculated as the average of T = 15 and T = 45. Before the submaximal exercise test, resting energy expenditure (REE) was measured using indirect calorimetry. The Weir equation[72] was used to calculate whole-body energy expenditure (EE). Net energy efficiency was computed as power output (watts converted to kJ/min) over EE during exercise (EEE) minus resting EE (REE) (Eq. 1) as described by[73].

Eq 1: NEE (%) = (Work (kJ/min)/ (EEE (kJ/min) – REE (kJ/min)) *100

Muscle strength
Muscle contractile performance was measured using the Biodex System 3 Pro dynamometer (Biodex® Medical Systems, Inc., Shirley, NY, USA). The participants were stabilized in the device with shoulder, leg, and abdominal straps to prevent compensatory movement for the measurements. The test was performed with the left leg in all participants. To measure maximal muscle strength, each participant performed 30 consecutive knee extension and flexion movements (range of motion 120 degrees/s). The peak torque of each extension and flexion was recorded. The maximal isokinetic knee-extensor and knee-flexor torque was defined as the highest peak torque and corrected for body weight (Nm/kg) and muscle volume (Nm/m^3).

Habitual physical activity
Habitual physical activity was determined in all participants using an ActivPAL monitor (PAL Technologies, Glasgow, Scotland) for a consecutive period of 5 days, including two weekend days. Besides the total amount of steps per day, the total stepping time was calculated in proportion to waking time, determined according to[74]. Stepping time (i. e., physical activity) was then further classified into high-intensity physical activity (HPA; minutes with a step frequency > 110 steps/min in proportion to waking time) and lower-intensity physical activity (LPA; minutes with a step frequency ≤ 110 steps/min in proportion to waking time)[38].

Metabolomics
Metabolomics was performed as previously described, with minor adjustments[75]. In a 2 mL tube, the following amounts of internal standard dissolved in water were added to each sample of approximately 5 mg of freeze-dried muscle tissue: adenosine-$^{15}N_5$-monophosphate (5 nmol), adenosine-$^{15}N_5$-triphosphate (5 nmol), D_4-alanine (0.5 nmol), D_7-arginine (0.5 nmol), D_3-aspartic acid (0.5 nmol), D_3-carnitine (0.5 nmol), D_4-citric acid

(0.5 nmol), $^{13}C_1$-citrulline (0.5 nmol), $^{13}C_6$-fructose-1,6-diphosphate (1 nmol), guanosine-$^{15}N_5$-monophosphate (5 nmol), guanosine-$^{15}N_5$-triphosphate (5 nmol), $^{13}C_6$-glucose (10 nmol), $^{13}C_6$-glucose-6-phosphate (1 nmol), D_3-glutamic acid (0.5 nmol), D_5-glutamine (0.5 nmol), D_5-glutathione (1 nmol), $^{13}C_6$-isoleucine (0.5 nmol), D_3-lactic acid (1 nmol), D_3-leucine (0.5 nmol), D_4-lysine (0.5 nmol), D_3-methionine (0.5 nmol), D_6-ornithine (0.5 nmol), D_5-phenylalanine (0.5 nmol), D_7-proline (0.5 nmol), $^{13}C_3$-pyruvate (0.5 nmol), D_3-serine (0.5 nmol), D_6-succinic acid (0.5 nmol), D5-tryptophan (0.5 nmol), D_4-tyrosine (0.5 nmol), D_8-valine (0.5 nmol). After adding the internal standard mix, a 5 mm stainless-steel bead and polar phase solvents (for a total of 500 µL water and 500 µL MeOH) were added and samples were homogenized using a TissueLyser II (Qiagen, Hilden, Germany) for 5 min at a frequency of 30 times/sec. Chloroform was added for a total of 1 mL to each sample before thorough mixing. Samples were then centrifuged for 10 minutes at 18.000*g*. The top layer, containing the polar phase, was transferred to a new 1.5 mL tube and dried using a vacuum concentrator at 60°C. Dried samples were reconstituted in 100 µL 3:2 (v/v) methanol:water. Metabolites were analyzed using a Waters Acquity ultra-high performance liquid chromatography system coupled to a Bruker Impact II™ Ultra-High Resolution Qq-Time-Of-Flight mass spectrometer. Samples were kept at 12°C during analysis and 5 µL of each sample was injected. Chromatographic separation was achieved using a Merck Millipore SeQuant ZIC-cHILIC column (PEEK 100 x 2.1 mm, 3 µm particle size). Column temperature was held at 30°C. Mobile phase consisted of (A) 1:9 (v/v) acetonitrile:water and (B) 9:1 (v/v) acetonitrile:water, both containing 5 mmol/L ammonium acetate. Using a flow rate of 0.25 mL/min, the LC gradient consisted of: 100% B for 0-2 min, reach 0% B at 28 min, 0% B for 28-30 min, reach 100% B at 31 min, 100% B for 31-32 min. Column re-equilibration is achieved at a flow rate of 0.4 mL/min at 100% B for 32-35 min. MS data were acquired using negative and positive ionization in full scan mode over the range of m/z 50-1200. Data were analyzed using Bruker TASQ software version 2.1.22.3. All reported metabolite intensities were normalized to dry tissue weight, as well as to internal standards with comparable retention times and response in the MS. Metabolite identification has been based on a combination of accurate mass, (relative) retention times and fragmentation spectra, compared to the analysis of a library of standards (Sigma-Aldrich MSMLS). General repeatability of metabolite analysis was assessed for each metabolite using repeated measurements of a pooled sample. Additionally, all peak integrations were manually checked for quality in each sample, as large natural variance may skew pooled sample results. For the detection of NAD^+ specifically, our MS semi-quantification is based on correction for a nitrogen ($^{15}N_5$) labeled ATP internal standard. Both NAD^+ and ATP contain several phosphate groups and the adenosine scaffold, resulting in them behaving in a very similar way throughout sample preparation, and furthermore, their retention times in the MS are generally within one minute of one another, making it more likely that they encounter similar matrix effects in the MS. We have previously demonstrated that this approach gives equivalent results as those performed using a dedicated enzymatic method for absolute NAD^+ quantification[27,76].

Statistical analyses and data visualization

Data was processed and analyses were performed with R version 3.5.1[77] and Bioconductor version 3.7[78]. Data was processed in part with the R package dplyr version 1.0.2[79]. Principal Component Analysis (PCA) was performed using the R package MixOmics version 6.6.2[80]. Significance was assessed using an empirical Bayes moderated t-test on log2 transformed data within limma's linear model framework, taking participant groups into account[81,82]. Networks were constructed and visualized using igraph version 1.2.4.2[83]. Unless implemented through an aforementioned R package or

base R graphics, visualization of data was performed using ggplot2 version 3.2.1[84], ggpubr v 0.2.5[85], ggrepel version 0.8.1[86], with colors from RColorBrewer version 1.1-2[87].

Data availability
Metabolomics data are available as supplementary materials accompanying this manuscript as both summary statistics and processed abundance values per individual (Supplemental Table 2). Physiological data from this cohort has been reported in our previous study as part of a different analysis[25]. All other data supporting the findings of this study are available from the corresponding author upon reasonable request.

Code availability
Code supporting the findings of this study are available from the corresponding author upon reasonable request

Acknowledgements
L.G., J.H. and P.S. are financially supported by the TIFN research program Mitochondrial Health (ALWTF.2015.5) and the Netherlands Organization for Scientific Research (NWO). Work in the Houtkooper group is financially supported by an ERC Starting grant (no. 638290), a VIDI grant from ZonMw (no. 91715305), and a grant from the Velux Stiftung (no. 1063). G.E.J. is supported by a VENI grant from ZonMw. R.Z-P is supported by a post-doctoral grant from the European Union's Horizon 2020 research and innovation program under the Marie Skłodowska-Curie grant agreement number 840110. The funders had no role in data collection and analysis, or decision to publish.

Author contributions
G.E.J., L.G., P.S., J.H., R.H.H. conceived the study. L.G. designed and performed the human cohort characterization and experiments. G.E.J designed and performed the bioinformatics analyses. R.Z-P, B.V.S and M.v.W. performed the metabolomics analyses. J.M.W.G. and J.d.V.d.B reviewed the manuscript**.** G.E.J., L.G., R.Z-P, B.V.S, P.S. R.H.H and J.H. interpreted the results and wrote the manuscript with contributions from all other authors.

Competing interests
J.M.W.G. and J.v.d.B are affiliated with FrieslandCampina and Danone Nutricia Research, respectively, which sponsored of the TIFN program and partly financed the project that led to human sample collection. They had no role in data collection, analysis, and decision to publish. The remaining authors declare no competing interests.

Figure Legends

A

	Young	Older adults		
		Trained	Normal	Impaired
Participants	12	17	17	6
Age range	20-30	65-80	65-80	65-80
Male (%)	58	65	53	50
BMI (kg/m²)	22.7	23.9	25.8	27
Steps/day	10153	13671	10197	6608
Time high activity (%)	2.5	5.2	2.2	1.0

B

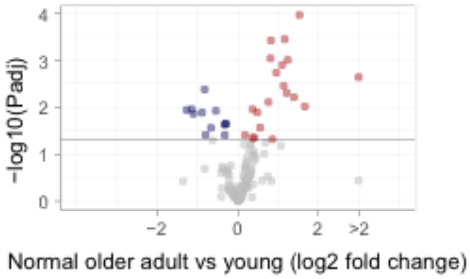

C

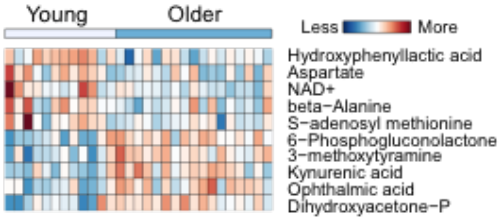

Figure 1: The metabolome of human muscle aging

(A) Study participants consisted of either young or older adults, whereby older adults were segmented into three categories: either 'exercise-trained,' 'normally physically active,' or 'physically impaired' with respect to their muscle health (Supplemental Table 1). Group averages are presented for BMI, steps-per-day, and high-intensity physical active time, **(B)** Volcano plot of fold change (x-axis, log2 scale) versus p-value (y-axis, -log10 scale) for older adults compared to young individuals with equal physical activity levels ('young' vs. 'normal older adults'), illustrating significantly depleted (blue) or accumulated (red) metabolites with age (comparing young, n=12, and normal older adults, n=17). The horizontal line indicates significance ($p<0.05$). Significance was determined using an empirical Bayes moderated t-test (two-sided, p values adjusted for multiple comparisons between groups)**. (C)** Top 5 accumulating and depleted metabolites in normal older adults compared to young, depicted as a heatmap with higher (red) or lower (blue) relative abundances of metabolites. Source data: supplemental Table 2.

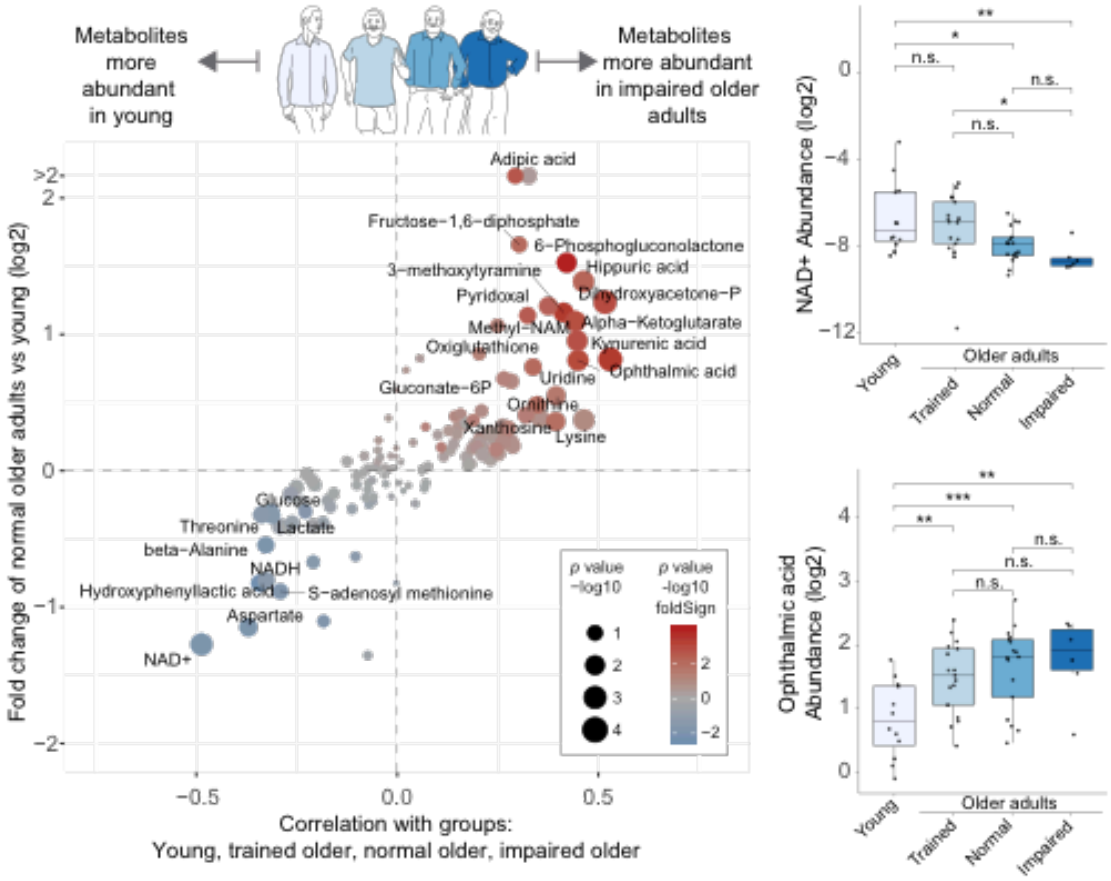

Figure 2: Muscle NAD$^+$ levels relate to muscle health during aging
(A) Comparison of: (x-axis) the correlation a metabolite has to the four muscle health groups (young adults, trained older adults, older adults with normal physical activity levels, and physically impaired older adults), where the size of point on the graph indicates p-value of the correlation (-log10 scale), and correlation and significance were determined using Pearson's product-moment correlation coefficient, and (y-axis) the fold change the metabolite undergoes in older vs. young adults with normal physical activity, where the color of the point indicates the p-value of aging fold change (with directionality represented as either increasing, red, or decreasing, blue) and significance was determined using an empirical Bayes moderated t-test (two-sided, p values adjusted for multiple comparisons between groups). The metabolite's name is depicted when the aging fold change had a significance of $p<0.05$. The graph reveals NAD$^+$ to be both depleted in aging and to follow the strongest correlation to a healthy aging trend. **(B)** Abundance levels of NAD$^+$ in the four muscle health groups. **(C)** Abundance levels of ophthalmic acid in the four muscle health groups. Sample sizes are: young n=12, older adults; trained n=17, normal=17, impaired=6. Significance was determined using an empirical Bayes moderated t-test (two-sided, p values adjusted for multiple comparisons between groups, * $p<0.05$, ** $p<0.01$, *** $p<0.001$, n.s. = not significant). Boxplots: Inner line within the box is the median of the data, the box extends to the upper and lower quartile of the dataset (25% of the data above and below the median), whiskers (dashed lines) represent up to 1.5 times the upper or lower quartiles, circles beyond the whisker represent individual data points outside this range. Source data: supplemental Table 2, all exact p values for comparison between groups are listed therein.

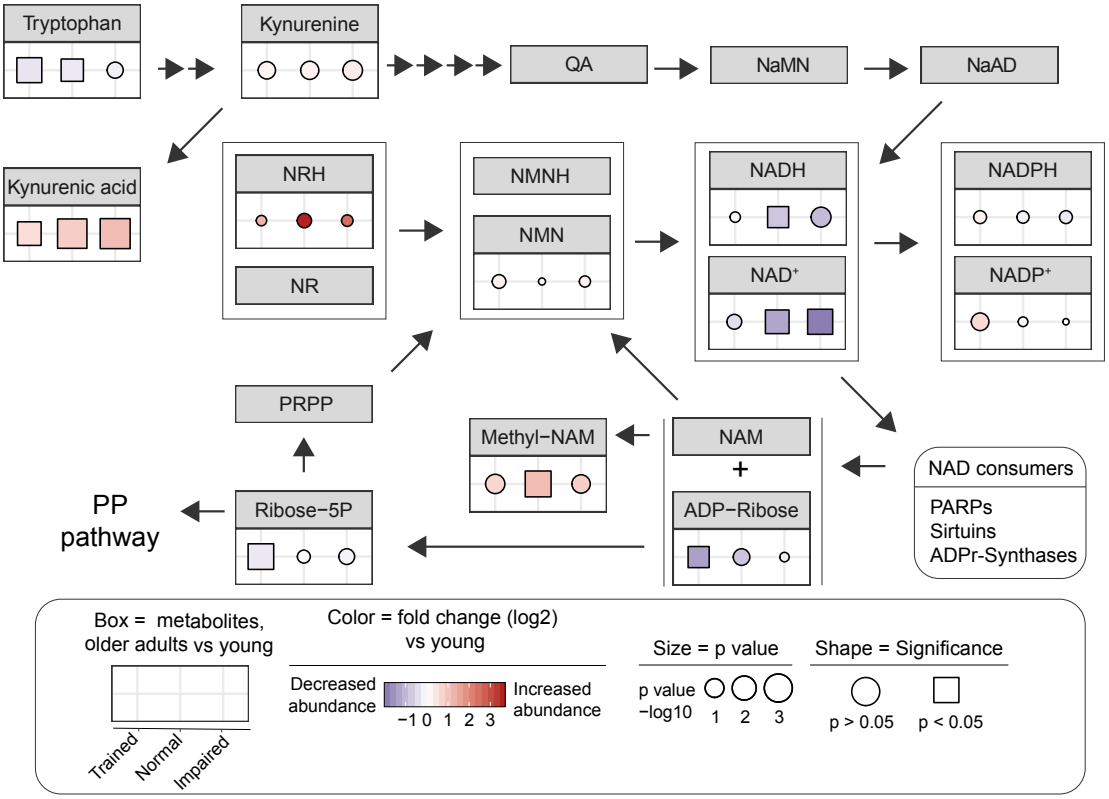

Figure 3: Major NAD$^+$ metabolites and changes in healthy muscle aging
Changes in the three older adult groups (trained, normally active, and physically impaired) relative to young are depicted for each NAD$^+$-related metabolite in the map. The color indicates the fold change (blue=decreased, red=increased), the size indicates the p-value of the significance (-log10 scale), and the shape denotes a significance threshold (square, $p<0.05$). Significance was determined using an empirical Bayes moderated t-test (two-sided, p values adjusted for multiple comparisons between groups). Source data: supplemental Table 2, all exact p values for comparison between groups are listed therein.

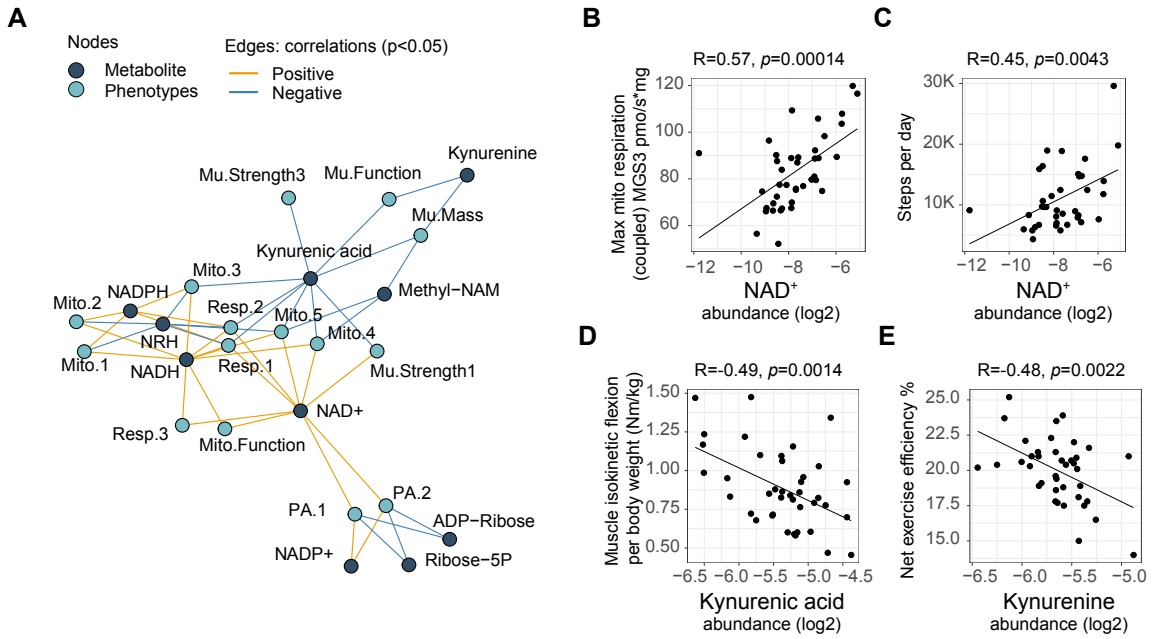

Figure 4: Molecular-physiological and NAD$^+$-related healthy aging network
(A) Network of significant associations between molecular-physiological parameters (light blue nodes) and NAD$^+$-related metabolites (dark blue nodes). Positive associations are in orange and negative associations in blue, where correlation and significance were determined in the older adults using Pearson's product-moment correlation coefficient ($p<0.05$). Sample size is all older adults (n=40). **(B-E)** Examples of correlations within the network, highlighting the positive associations between **(B)** NAD$^+$ and mitochondrial respiration (R=0.57, p=0.00014), and **(C)** NAD$^+$ and average daily steps, and highlighting the negative associations between (R=0.45, p=0.0043) **(D)** Kynurenic acid and muscle strength (R=-0.49, p=0.0014) and **(E)** Kynurenine and exercise efficiency (R=-0.48, p=0.0022). Sample size is all older adults (n=40) and p value is significance of Pearson's product-moment correlation coefficient. Source data: supplemental Table 2 and physiological data is available in our previous study[25].

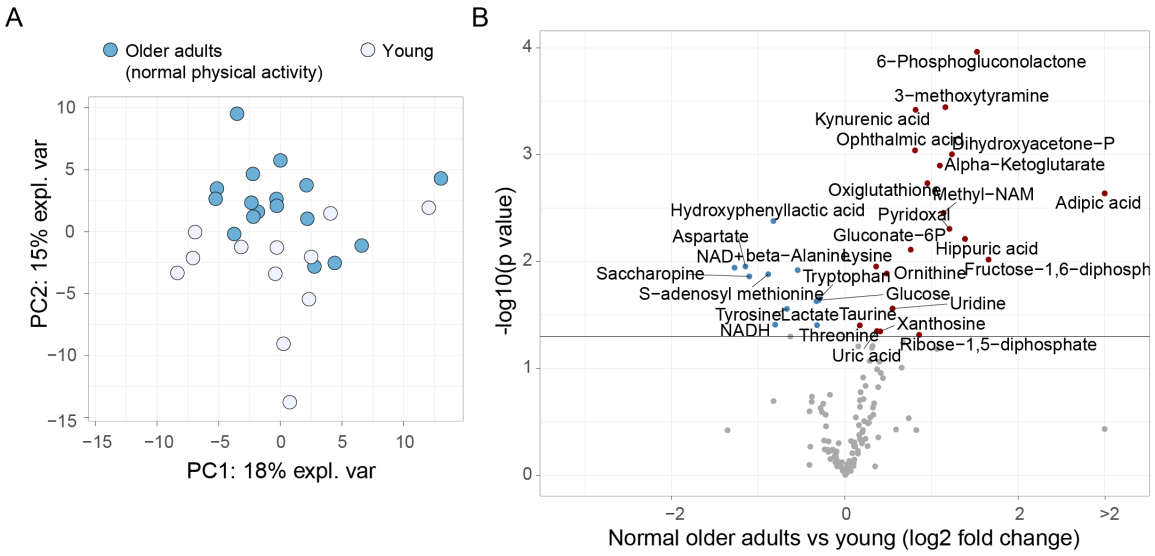

Extended data figure 1: Global metabolomics changes of human muscle aging. (A) Principal Component Analysis (PCA) of metabolomes of young and older individuals possessing equal physical activity levels ('young' vs 'normal older adults'). (B) Volcano plot of fold change (x-axis, log2 scale) versus p-value (y-axis, -log10 scale) for older adults (n=17) compared to young individuals (n=12) with equal physical activity levels, illustrating significantly lower (blue) or higher (red) metabolites with age. The horizontal line indicates significance (p<0.05). Significance was determined using an empirical Bayes moderated t-test (two-sided, p values adjusted for multiple comparisons between groups). Source data: supplemental Table 2, all exact p values for comparison between groups are listed therein.

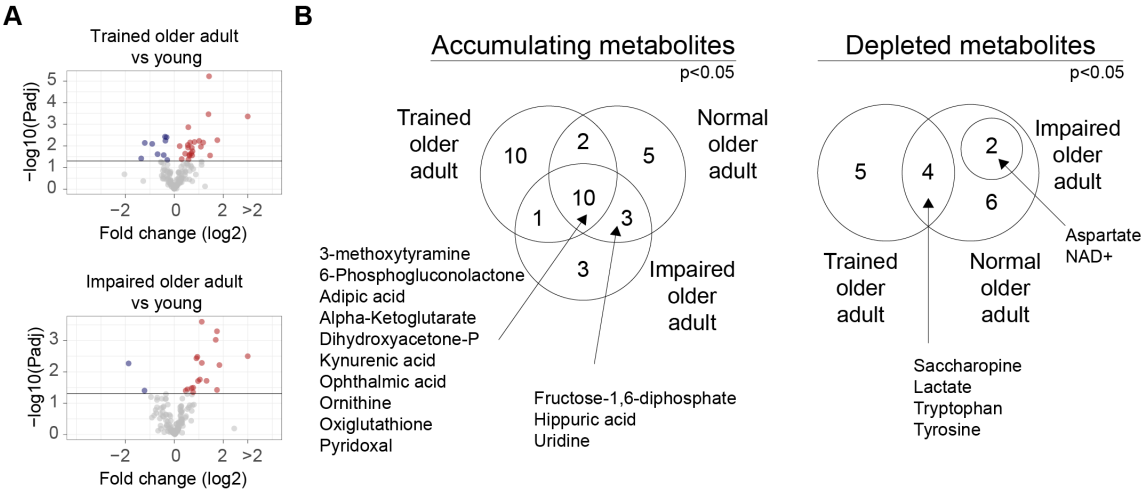

Extended data figure 2: Comparison of age-related changes in each aging group. (A) Volcano plots of fold change (x-axis, log2 scale) versus p-value (y-axis, -log10 scale) for trained older adults (top; n=17), and physically impaired older adults (bottom; n=6) compared to young individuals (n=12), illustrating significantly depleted (blue) or accumulated (red) metabolites with age. Line indicates significance (p<0.05). Significance was determined using an empirical Bayes moderated t-test (two-sided, p values adjusted for multiple comparisons between groups). (B) Venn diagram of the

overlap of significantly higher or lower abundances of metabolites in each aged group (trained older adults, older adults with normal physical activity levels, physically impaired older adults) compared to young individuals ($p < 0.05$). Source data: supplemental Table 2, all exact p values for comparison between groups are listed therein.

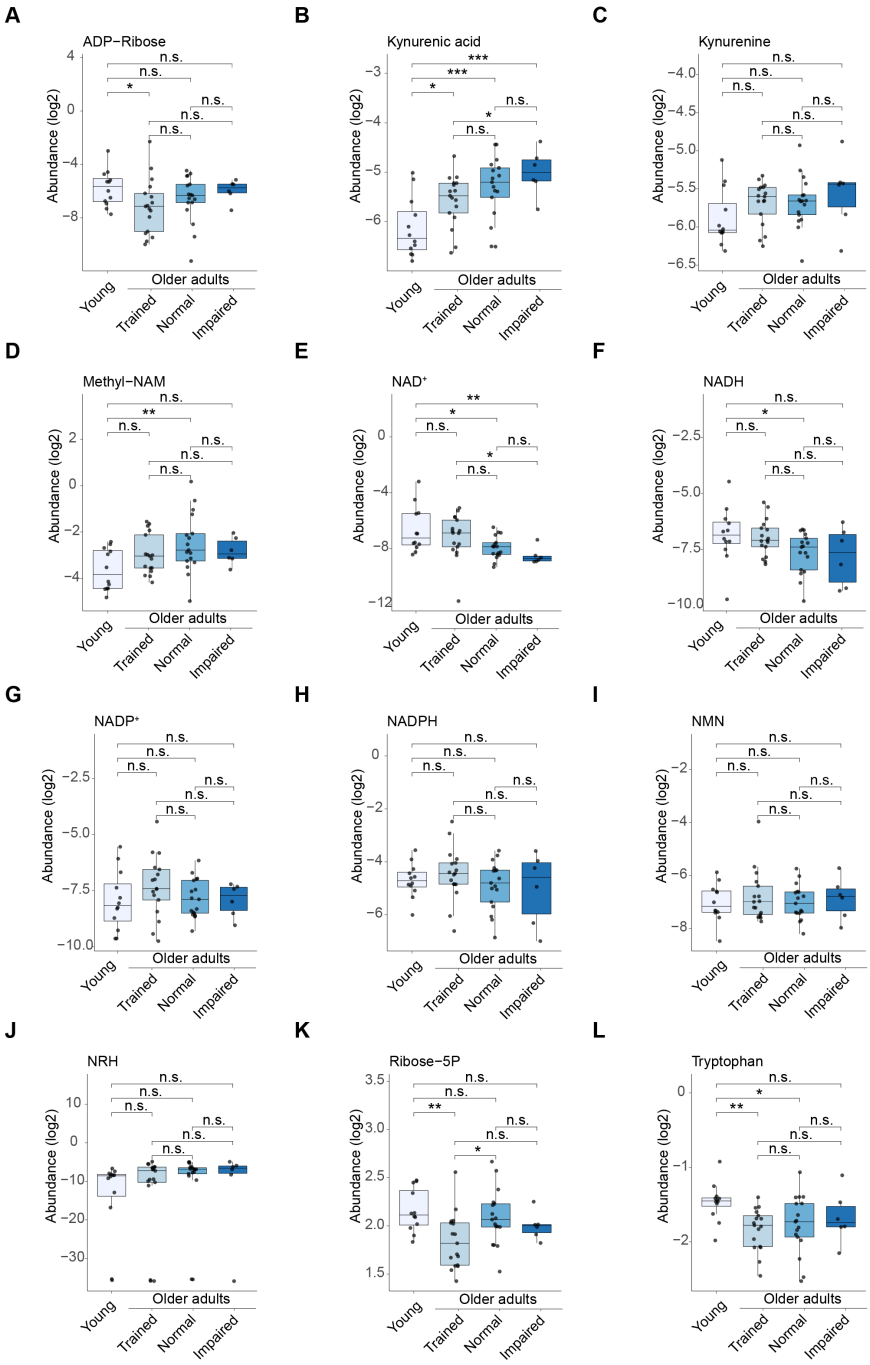

Extended data figure 3: NAD$^+$-related metabolites of healthy aging groups. (A-L) Abundance levels of NAD+-related metabolites in the four muscle health groups, for (A) ADP-ribose, (B) Kynurenic acid, (C) Kynurenine, (D) Methyl-NAM, (E) NAD+, (F) NADH, (G) NADP+, (H) NADPH, (I) Nicotinamide mononucleotide (NMN), (J)

Dihydronicotinamide riboside (NRH), (K) Ribose-5P, and (L) Tryptophan. Sample sizes are: young n=12, older adults; trained n=17, normal=17, impaired=6. Significance was determined using an empirical Bayes moderated t-test (two-sided, p values adjusted for multiple comparisons between groups, * p<0.05, ** p<0.01, *** p<0.001, n.s. = not significant). Boxplots: Inner line within the box is the median of the data, the box extends to the upper and lower quartile of the dataset (25% of the data above and below the median), whiskers (dashed lines) represent up to 1.5 times the upper or lower quartiles, circles beyond the whisker represent individual data points outside this range. Source data: supplemental Table 2, all exact p values for comparison between groups are listed therein.

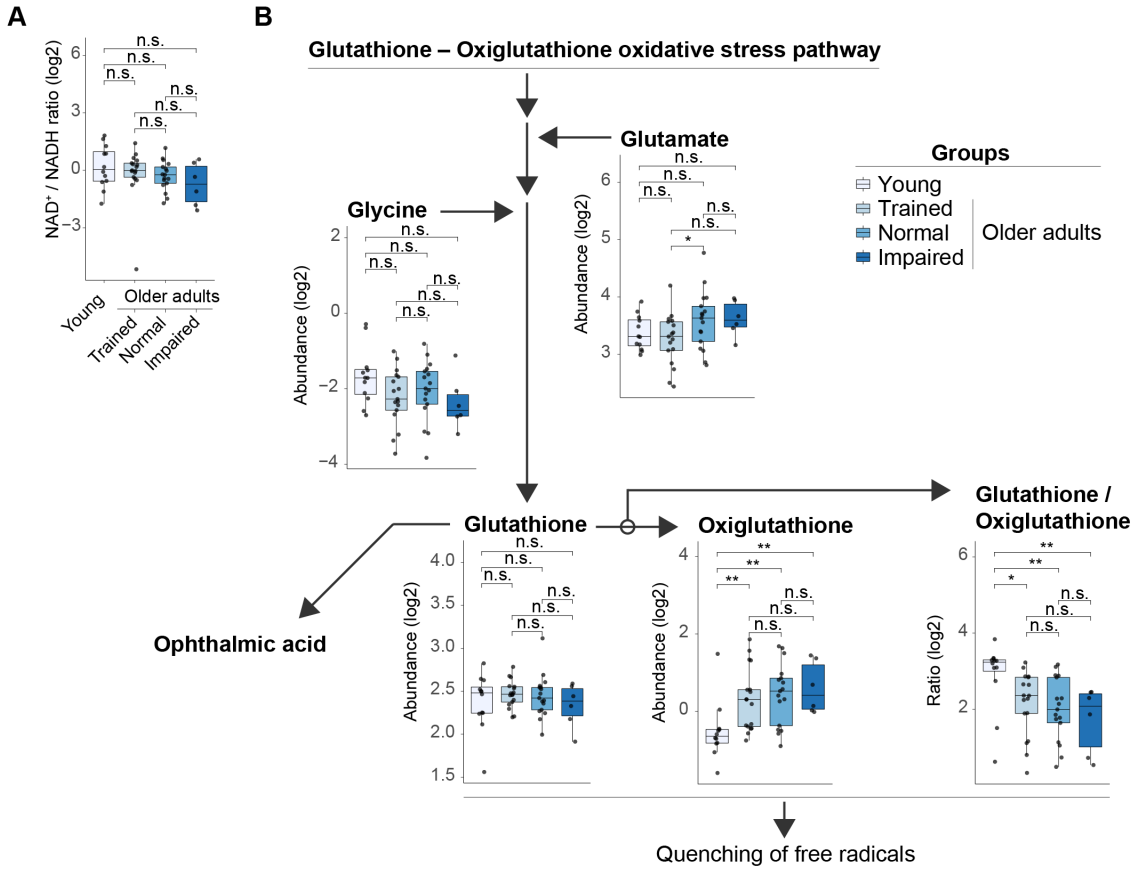

Extended data figure 4: NAD$^+$ – NADH ratio, and the glutathione – oxiglutathion oxidative stress pathway. (A) NAD+ to NADH ratio (log2 scale) in young and older adults belonging to trained, normal, and impaired aging groups. (B) The glutathione – oxliglutathione oxidative stress pathway for metabolites measured in this study. Glutamate and glycine feed into glutathione production. Conversion of glutathione to oxiglutathione results in quenching of free radicals, whereby the ratio of glutathione to oxiglutathione is indicative of this process. A byproduct of this pathway is ophthalmic acid (data presented in Figure 2C). Data suggests an increase of the oxidative milieu in the aged groups relative to young. Sample sizes are: young n=12, older adults; trained n=17, normal=17, impaired=6. Significance was determined using an empirical Bayes moderated t-test (two-sided, p values adjusted for multiple comparisons between groups, * p<0.05, ** p<0.01, n.s. = not significant). Boxplots: Inner line within the box is the median of the data, the box extends to the upper and lower quartile of the dataset

(25% of the data above and below the median), whiskers (dashed lines) represent up to 1.5 times the upper or lower quartiles, circles beyond the whisker represent individual data points outside this range. Source data: supplemental Table 2, all exact p values for comparison between groups are listed therein.

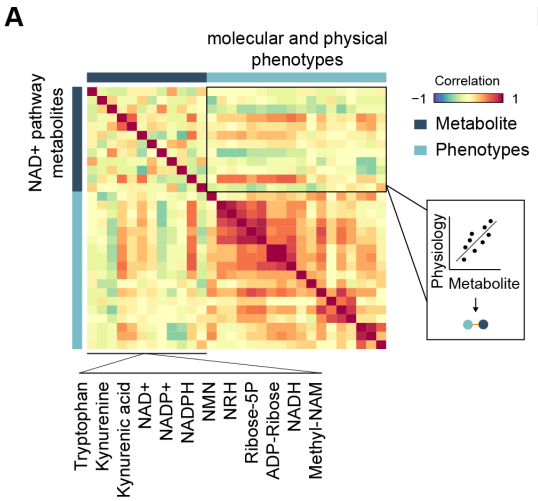

B

Node	Measurement
Mu.Function	Muscle function - Net exercise efficiency (%)
Mito.1	Mitochondria - OXPHOS compl V blot (A.U.)
Mito.2	Mitochondria - OXPHOS compl III blot (A.U.)
Mito.3	Mitochondria - OXPHOS compl II blot (A.U.)
Mito.4	Mitochondria - OXPHOS compl IV blot (A.U.)
Mito.5	Mitochondria - OXPHOS compl I blot (A.U.)
Resp.1	Respiration - Coupled MOGS3 (pmol/(s*mg))
Resp.2	Respiration - Uncoupled MOGS (pmol/(s*mg))
Resp.3	Respiration - Coupled MGS3 (pmol/(s*mg))
Mito.Function	Mitochondrial function - MRS PCr recovery rate
Mu.Mass	Muscle mass - MRI Muscle volume (cm3)
Mu.Strength1	Muscle isokinetic extension / body weight (Nm/kg)
Mu.Strength2	Muscle isokinetic extension / muscle volume (Nm/cm3)
Mu.Strength3	Muscle isokinetic flexion / body weight (Nm/kg)
Mu.Strength4	Muscle isokinetic flexion / muscle volume (Nm/cm3)
PA.1	Physical activity - steps per day
PA.2	Physical activity- % time high physical activity
PA.3	Physical activity- % time low physical activity

Extended data figure 5: Correlation of molecular-physiological phenotypes with metabolites involved in NAD$^+$ synthesis. (A) Correlation matrix comparing the paired metabolome (dark blue) and muscle health parameters (light blue) in the older adults (Pearson's product-moment correlation coefficient, sample size is all older adults, n=40). The scale ranges from blue (negative correlation), to yellow (no correlation), to red (positive correlation). Inset and cartoon: correlation between metabolites and muscle health parameters are used to reconstruct the network. (B) Abbreviations and measurements of the molecular-physiological phenotypes assessed in this analysis. Note: MOGS3, state 3 respiration upon malate + octanoyl-carnitine + glutamate + succinate, MGS3, state 3 respiration upon malate + glutamate + succinate. Source data: supplemental Table 2 and physiological data is available in our previous study[25].

References

1. Salomon, J. A. *et al.* Healthy life expectancy for 187 countries, 1990-2010: A systematic analysis for the Global Burden Disease Study 2010. *Lancet* (2012). doi:10.1016/S0140-6736(12)61690-0
2. Ferrucci, L., Giallauria, F. & Guralnik, J. M. Epidemiology of Aging. *Radiologic Clinics of North America* (2008). doi:10.1016/j.rcl.2008.07.005
3. Butler, R. N. *et al.* New model of health promotion and disease prevention for the 21st century. *BMJ* (2008). doi:10.1136/bmj.a399
4. Niccoli, T. & Partridge, L. Ageing as a risk factor for disease. *Current Biology* **22**, (2012).
5. López-Otín, C., Blasco, M. A., Partridge, L., Serrano, M. & Kroemer, G. The hallmarks of aging. *Cell* **153**, (2013).
6. Houtkooper, R. H. *et al.* The metabolic footprint of aging in mice. *Sci. Rep.* **1**, 134 (2011).
7. Uchitomi, R. *et al.* Metabolomic Analysis of Skeletal Muscle in Aged Mice. *Sci. Rep.* (2019). doi:10.1038/s41598-019-46929-8

8. Gao, A. W. *et al.* A sensitive mass spectrometry platform identifies metabolic changes of life history traits in C. elegans. *Sci. Rep.* **7**, (2017).
9. Roubenoff, R. Sarcopenia and its implications for the elderly. *Eur. J. Clin. Nutr.* (2000). doi:10.1038/sj.ejcn.1601024
10. Janssen, I., Heymsfield, S. B. & Ross, R. Low relative skeletal muscle mass (sarcopenia) in older persons is associated with functional impairment and physical disability. *J. Am. Geriatr. Soc.* (2002). doi:10.1046/j.1532-5415.2002.50216.x
11. Distefano, G. *et al.* Physical activity unveils the relationship between mitochondrial energetics, muscle quality, and physical function in older adults. *J. Cachexia. Sarcopenia Muscle* (2018). doi:10.1002/jcsm.12272
12. Talbot, L. A., Musiol, R. J., Witham, E. K. & Metter, E. J. Falls in young, middle-aged and older community dwelling adults: Perceived cause, environmental factors and injury. *BMC Public Health* (2005). doi:10.1186/1471-2458-5-86
13. Gadelha, A. B., Neri, S. G. R., Bottaro, M. & Lima, R. M. The relationship between muscle quality and incidence of falls in older community-dwelling women: An 18-month follow-up study. *Exp. Gerontol.* (2018). doi:10.1016/j.exger.2018.06.018
14. Fried, L. P. *et al.* Frailty in older adults: Evidence for a phenotype. *Journals Gerontol. - Ser. A Biol. Sci. Med. Sci.* (2001). doi:10.1093/gerona/56.3.m146
15. Amati, F. *et al.* Physical inactivity and obesity underlie the insulin resistance of aging. *Diabetes Care* (2009). doi:10.2337/dc09-0267
16. Riera, C. E. & Dillin, A. Tipping the metabolic scales towards increased longevity in mammals. *Nat. Cell Biol.* **17**, 196–203 (2015).
17. Romani, M. *et al.* NAD+ boosting reduces age-associated amyloidosis and restores mitochondrial homeostasis in muscle. *Cell Rep.* **34**, 108660 (2021).
18. Cartee, G. D., Hepple, R. T., Bamman, M. M. & Zierath, J. R. Exercise Promotes Healthy Aging of Skeletal Muscle. *Cell Metabolism* **23**, 1034–1047 (2016).
19. Greggio, C. *et al.* Enhanced Respiratory Chain Supercomplex Formation in Response to Exercise in Human Skeletal Muscle. *Cell Metab.* **25**, 301–311 (2017).
20. Soga, T. *et al.* Differential metabolomics reveals ophthalmic acid as an oxidative stress biomarker indicating hepatic glutathione consumption. *J. Biol. Chem.* (2006). doi:10.1074/jbc.M601876200
21. Dello, S. A. W. G. *et al.* Systematic review of ophthalmate as a novel biomarker of hepatic glutathione depletion. *Clinical Nutrition* (2013). doi:10.1016/j.clnu.2012.10.008
22. Smith, K. R., Hayat, F., Andrews, J. F., Migaud, M. E. & Gassman, N. R. Dihydroxyacetone Exposure Alters NAD(P)H and Induces Mitochondrial Stress and Autophagy in HEK293T Cells. *Chem. Res. Toxicol.* (2019). doi:10.1021/acs.chemrestox.9b00230
23. Gluck, M. R. & Zeevalk, G. D. Inhibition of brain mitochondrial respiration by dopamine and its metabolites: Implications for Parkinson's disease and catecholamine-associated diseases. *J. Neurochem.* (2004). doi:10.1111/j.1471-4159.2004.02747.x
24. Wirthgen, E., Hoeflich, A., Rebl, A. & Günther, J. Kynurenic Acid: The Janus-faced role of an immunomodulatory tryptophan metabolite and its link to pathological conditions. *Frontiers in Immunology* (2018). doi:10.3389/fimmu.2017.01957
25. Grevendonk, L. *et al.* Impact of aging and exercise on skeletal muscle mitochondrial capacity, energy metabolism, and physical function. *Nat. Commun.* **12**, 1–17 (2021).

26. Rajman, L., Chwalek, K. & Sinclair, D. A. Therapeutic Potential of NAD-Boosting Molecules: The In Vivo Evidence. *Cell Metabolism* (2018). doi:10.1016/j.cmet.2018.02.011
27. Remie, C. M. E. *et al.* Nicotinamide riboside supplementation alters body composition and skeletal muscle acetylcarnitine concentrations in healthy obese humans. *Am. J. Clin. Nutr.* (2020). doi:10.1093/ajcn/nqaa072
28. Pirinen, E. *et al.* Clinical and Translational Report Niacin Cures Systemic NAD + Deficiency and Improves Muscle Performance in Adult-Onset Mitochondrial Myopathy Niacin Cures Systemic NAD + Deficiency and Improves Muscle Performance in Adult-Onset Mitochondrial Myopathy. *Cell Metab.* **31**, (2020).
29. Elhassan, Y. S. *et al.* Nicotinamide Riboside Augments the Aged Human Skeletal Muscle NAD+ Metabolome and Induces Transcriptomic and Anti-inflammatory Signatures. *Cell Rep.* **28**, 1717-1728.e6 (2019).
30. Cantó, C. *et al.* The NAD+ precursor nicotinamide riboside enhances oxidative metabolism and protects against high-fat diet-induced obesity. *Cell Metab.* (2012). doi:10.1016/j.cmet.2012.04.022
31. Sorrentino, V. *et al.* Enhancing mitochondrial proteostasis reduces amyloid-β proteotoxicity. *Nature* **552**, 187–193 (2017).
32. Zhang, H. *et al.* NAD+ repletion improves mitochondrial and stem cell function and enhances life span in mice. *Science (80-.).* (2016). doi:10.1126/science.aaf2693
33. Gomes, A. P. *et al.* Declining NAD+ induces a pseudohypoxic state disrupting nuclear-mitochondrial communication during aging. *Cell* (2013). doi:10.1016/j.cell.2013.11.037
34. Mills, K. F. *et al.* Long-Term Administration of Nicotinamide Mononucleotide Mitigates Age-Associated Physiological Decline in Mice. *Cell Metab.* (2016). doi:10.1016/j.cmet.2016.09.013
35. Yoshino, J., Mills, K. F., Yoon, M. J. & Imai, S. I. Nicotinamide mononucleotide, a key NAD + intermediate, treats the pathophysiology of diet- and age-induced diabetes in mice. *Cell Metab.* (2011). doi:10.1016/j.cmet.2011.08.014
36. Mouchiroud, L. *et al.* The NAD+/sirtuin pathway modulates longevity through activation of mitochondrial UPR and FOXO signaling. *Cell* (2013). doi:10.1016/j.cell.2013.06.016
37. Connell, N. J., Houtkooper, R. H. & Schrauwen, P. NAD + metabolism as a target for metabolic health: have we found the silver bullet? *Diabetologia* (2019). doi:10.1007/s00125-019-4831-3
38. Tudor-Locke, C. *et al.* How many steps/day are enough? for adults. *Int. J. Behav. Nutr. Phys. Act.* (2011). doi:10.1186/1479-5868-8-79
39. Tudor-Locke, C., Hatano, Y., Pangrazi, R. P. & Kang, M. Revisiting 'how many steps are enough?' *Med. Sci. Sports Exerc.* (2008). doi:10.1249/MSS.0b013e31817c7133
40. Zhu, X. H., Lu, M., Lee, B. Y., Ugurbil, K. & Chen, W. In vivo NAD assay reveals the intracellular NAD contents and redox state in healthy human brain and their age dependences. *Proc. Natl. Acad. Sci. U. S. A.* (2015). doi:10.1073/pnas.1417921112
41. Cuenoud, B. *et al.* Brain NAD Is Associated With ATP Energy Production and Membrane Phospholipid Turnover in Humans. *Front. Aging Neurosci.* (2020). doi:10.3389/fnagi.2020.609517
42. Massudi, H. *et al.* Age-associated changes in oxidative stress and NAD+ metabolism in human tissue. *PLoS One* (2012). doi:10.1371/journal.pone.0042357

43. de Guia, R. M. *et al.* Aerobic and resistance exercise training reverses age-dependent decline in NAD+ salvage capacity in human skeletal muscle. *Physiol. Rep.* (2019). doi:10.14814/phy2.14139
44. Drummond, M. J. *et al.* Aging and microRNA expression in human skeletal muscle: A microarray and bioinformatics analysis. *Physiol. Genomics* (2011). doi:10.1152/physiolgenomics.00148.2010
45. Fazelzadeh, P. *et al.* The Muscle Metabolome Differs between Healthy and Frail Older Adults. *J. Proteome Res.* (2016). doi:10.1021/acs.jproteome.5b00840
46. Rivas, D. A. *et al.* Diminished skeletal muscle microRNA expression with aging is associated with attenuated muscle plasticity and inhibition of IGF-1 signaling. *FASEB J.* (2014). doi:10.1096/fj.14-254490
47. Migliavacca, E. *et al.* Mitochondrial oxidative capacity and NAD+ biosynthesis are reduced in human sarcopenia across ethnicities. *Nat. Commun.* (2019). doi:10.1038/s41467-019-13694-1
48. Costford, S. R. *et al.* Skeletal muscle NAMPT is induced by exercise in humans. *Am. J. Physiol. - Endocrinol. Metab.* (2010). doi:10.1152/ajpendo.00318.2009
49. Zha, M. *et al.* Molecular Mechanism of ADP-Ribose Hydrolysis By Human NUDT5 From Structural and Kinetic Studies. *J. Mol. Biol.* (2008). doi:10.1016/j.jmb.2008.04.006
50. Perraud, A. L. *et al.* NUDT9, a member of the Nudix hydrolase family, is an evolutionarily conserved mitochondrial ADP-ribose pyrophosphatase. *J. Biol. Chem.* (2003). doi:10.1074/jbc.M205601200
51. Hove-Jensen, B. *et al.* Phosphoribosyl Diphosphate (PRPP): Biosynthesis, Enzymology, Utilization, and Metabolic Significance. *Microbiol. Mol. Biol. Rev.* (2017). doi:10.1128/mmbr.00040-16
52. Kepplinger, B. *et al.* Age-related increase of kynurenic acid in human cerebrospinal fluid - IgG and β2-microglobulin changes. *NeuroSignals* (2005). doi:10.1159/000086295
53. Vohra, M., Lemieux, G. A., Lin, L. & Ashrafi, K. Kynurenic acid accumulation underlies learning and memory impairment associated with aging. *Genes Dev.* (2018). doi:10.1101/gad.307918.117
54. Calder, P. C. *et al.* Health relevance of the modification of low grade inflammation in ageing (inflammageing) and the role of nutrition. *Ageing Research Reviews* (2017). doi:10.1016/j.arr.2017.09.001
55. Lim, A., Harijanto, C., Vogrin, S., Guillemin, G. & Duque, G. Does Exercise Influence Kynurenine/Tryptophan Metabolism and Psychological Outcomes in Persons With Age-Related Diseases? A Systematic Review. *International Journal of Tryptophan Research* (2021). doi:10.1177/1178646921991119
56. Sorgdrager, F. J. H., Naudé, P. J. W., Kema, I. P., Nollen, E. A. & De Deyn, P. P. Tryptophan metabolism in inflammaging: From biomarker to therapeutic target. *Frontiers in Immunology* (2019). doi:10.3389/fimmu.2019.02565
57. Agudelo, L. Z. *et al.* Skeletal muscle PGC-1α1 reroutes kynurenine metabolism to increase energy efficiency and fatigue-resistance. *Nat. Commun.* (2019). doi:10.1038/s41467-019-10712-0
58. Yoshino, M. *et al.* Nicotinamide mononucleotide increases muscle insulin sensitivity in prediabetic women. *Science (80-.).* (2021). doi:10.1126/science.abe9985
59. Moore, M. P. & Mucinski, J. M. Impact of nicotinamide riboside supplementation on skeletal muscle mitochondria and whole-body glucose homeostasis: challenging the current hypothesis. *Journal of Physiology* (2020). doi:10.1113/JP279749

60. Aagaard, P., Magnusson, P. S., Larsson, B., Kjær, M. & Krustrup, P. Mechanical muscle function, morphology, and fiber type in lifelong trained elderly. *Med. Sci. Sports Exerc.* (2007). doi:10.1249/mss.0b013e31814fb402
61. Mackey, A. L. *et al.* Differential satellite cell density of type I and II fibres with lifelong endurance running in old men. *Acta Physiol.* (2014). doi:10.1111/apha.12195
62. Mosole, S. *et al.* Long-term high-level exercise promotes muscle reinnervation with age. *J. Neuropathol. Exp. Neurol.* (2014). doi:10.1097/NEN.0000000000000032
63. Di Lisa, F. & Ziegler, M. Pathophysiological relevance of mitochondria in NAD+ metabolism. *FEBS Letters* (2001). doi:10.1016/S0014-5793(01)02198-6
64. Guralnik, J. M. *et al.* A short physical performance battery assessing lower extremity function: Association with self-reported disability and prediction of mortality and nursing home admission. *Journals Gerontol.* (1994). doi:10.1093/geronj/49.2.M85
65. Bergström, J., Hermansen, L., Hultman, E. & Saltin, B. Diet, Muscle Glycogen and Physical Performance. *Acta Physiol. Scand.* (1967). doi:10.1111/j.1748-1716.1967.tb03720.x
66. Phielix, E. *et al.* Lower intrinsic ADP-stimulated mitochondrial respiration underlies in vivo mitochondrial dysfunction in muscle of male type 2 diabetic patients. *Diabetes* (2008). doi:10.2337/db08-0391
67. Boushel, R. *et al.* Patients with type 2 diabetes have normal mitochondrial function in skeletal muscle. *Diabetologia* (2007). doi:10.1007/s00125-007-0594-3
68. Hoeks, J. *et al.* Prolonged fasting identifies skeletal muscle mitochondrial dysfunction as consequence rather than cause of human insulin resistance. *Diabetes* (2010). doi:10.2337/db10-0519
69. van Moorsel, D. *et al.* Demonstration of a day-night rhythm in human skeletal muscle oxidative capacity. *Mol. Metab.* (2016). doi:10.1016/j.molmet.2016.06.012
70. Schrauwen-Hinderling, V. B. *et al.* Impaired in vivo mitochondrial function but similar intramyocellular lipid content in patients with type 2 diabetes mellitus and BMI-matched control subjects. *Diabetologia* (2007). doi:10.1007/s00125-006-0475-1
71. Kemp, G. J. & Radda, G. K. Quantitative interpretation of bioenergetic data from 31P and 1H magnetic resonance spectroscopic studies of skeletal muscle: an analytical review. *Magnetic resonance quarterly* (1994).
72. Weir, J. B. d. V. New methods for calculating metabolic rate with special reference to protein metabolism. *J. Physiol.* (1949). doi:10.1113/jphysiol.1949.sp004363
73. Matomäki, P., Linnamo, V. & Kyröläinen, H. A Comparison of Methodological Approaches to Measuring Cycling Mechanical Efficiency. *Sport. Med. - Open* (2019). doi:10.1186/s40798-019-0196-x
74. van der Berg, J. D. *et al.* Identifying waking time in 24-h accelerometry data in adults using an automated algorithm. *J. Sports Sci.* (2016). doi:10.1080/02640414.2016.1140908
75. Molenaars, M. *et al.* A Conserved Mito-Cytosolic Translational Balance Links Two Longevity Pathways. *Cell Metab.* (2020). doi:10.1016/j.cmet.2020.01.011
76. Zapata-Pérez, R. *et al.* Reduced nicotinamide mononucleotide is a new and potent nad+ precursor in mammalian cells and mice. *FASEB J.* (2021). doi:10.1096/fj.202001826R
77. The R Development Core Team. R: A language and environment for statistical computing. *R Foundation for Statistical Computing* Vienna, Austria. ISBN 3-900051-07-0, URL http://ww (2010).

78. Gentleman, R. C. *et al.* Bioconductor: open software development for computational biology and bioinformatics. *Genome Biol.* (2004). doi:10.1186/gb-2004-5-10-r80
79. Wickham, H., François, R., Henry, L. & Müller, K. dplyr: A Grammar of Data Manipulation. R package version. *Media* (2019).
80. Rohart, F., Gautier, B., Singh, A. & Lê Cao, K. A. mixOmics: An R package for 'omics feature selection and multiple data integration. *PLoS Comput. Biol.* **13**, e1005752 (2017).
81. Ritchie, M. E. *et al.* limma powers differential expression analyses for RNA-sequencing and microarray studies. *Nucleic Acids Res.* **43**, e47 (2015).
82. Law, C. W., Chen, Y., Shi, W. & Smyth, G. K. voom: Precision weights unlock linear model analysis tools for RNA-seq read counts. *Genome Biol.* **15**, R29 (2014).
83. Csardi, G. & Nepusz, T. The igraph software package for complex network research. *InterJournal* **Complex Sy**, 1695 (2006).
84. Wickham, H. Ggplot2. *Wiley Interdiscip. Rev. Comput. Stat.* **3**, 180–185 (2011).
85. Kassambara, A. Package 'ggpubr': 'ggplot2' Based Publication Ready Plots. *R Packag. version 0.4.0* (2020).
86. Slowikowski, K. ggrepel: Automatically Position Non-Overlapping Text Labels with 'ggplot2'. *R package version 0.8.2* (2020).
87. Neuwirth, E. RColorBrewer: ColorBrewer palettes. *R Packag. version 1.1-2* https://cran.R-project.org/package=RColorBrewer (2014).